Efficient simulated tempering with approximated weights: Applications to first-order phase transitions

A. Valentim,[1] Claudio J. DaSilva,[2] and Carlos E. Fiore[3,*]

[1] *Departamento de Física, Universidade Federal do Paraná, CP 19044, 81531-980 Curitiba-PR, Brazil*
[2] *Instituto Federal de Educação, Ciência e Tecnologia de Goiás, C.P. 74130-012, Goiânia, Goiás, Brazil*
[3] *Instituto de Física, Universidade de São Paulo, C. P. 66318 05315-970 São Paulo, São Paulo, Brazil*

(Dated: August 11, 2015)

Simulated tempering (ST) has attracted a great deal of attention in the last years, due to its capability to allow systems with complex dynamics to escape from regions separated by large entropic barriers. However its performance is strongly dependent on basic ingredients, such as the choice of the set of temperatures and their associated weights. Since the weight evaluations are not trivial tasks, an alternative approximated approach was proposed by Park and Pande (Phys. Rev. E **76**, 016703 (2007)) to circumvent this difficulty. Here we present a detailed study about this procedure by comparing its performance with exact (free-energy) weights and other methods, its dependence on the total replica number R and on the temperature set. The ideas above are analyzed in four distinct lattice models presenting strong first-order phase transitions, hence constituting ideal examples in which the performance of algorithm is fundamental. In all cases, our results reveal that approximated weights work properly in the regime of larger R's. On the other hand, for sufficiently small R its performance is reduced and the systems do not cross properly the free-energy barriers. Finally, for estimating reliable temperature sets, we consider a simple protocol proposed at Comp. Phys. Comm. **128**, 2046 (2014).

PACS numbers: 05.10.Ln, 05.70.Fh, 05.50.+q

I. INTRODUCTION

Although Monte Carlo method has become probably the most common tool for studying phase transitions and critical phenomena, in practice its usage is not so simple, whenever standard algorithms (e.g. Metropolis) are used. Despite the simplicity and generality, they lead to difficulties close to the emergence of phase transitions. For instance, alternative procedures are typically required, specially in the case of systems with microscopic configurations separated by valleys and hills in the free-energy landscape [1–4]. Cluster algorithms [5, 6], multicanonical [7], Wang-Landau [8] and tempering methods are some examples of proposals to overcome these difficulties. In particular, parallel tempering (PT) [9] and simulated tempering (ST) [10] enhanced sampling methods have drawn attention due to their generality and simplicity when compared with the previous examples. Their basic idea consists of using configurations from high temperatures for systems at low temperatures, allowing in principle the dynamics to escape from metastable states and providing an appropriate visit of the configuration space. In particular, distinct aspects of tempering methods have been explored in the last years, aiming at better understanding of efficiency and pertinence. For instance, the role of temperature sets for the PT case was investigated in Refs. [11–14], whilst the importance of non-adjacent exchanges was taken into account in Refs. [14–18]. In addition the efficiency and comparison between tempering methods were considered in Refs. [19–21].

Focusing our attention in the ST we face one of its main difficulties, namely the evaluation of the free-energy weights, required for an uniform sampling to all temperatures. Despite the development of alternative techniques, their applicability for more complex systems still poses a hardship. In some cases [21, 22], the accumulation of histograms (of a given quantity) and previous simulations are necessary to calculate (or to estimate) the input parameters that guarantee a sufficient number of visits to all temperatures. In such cases, the weights are set arbitrarily but a knowledge of the partition function Z_i at each temperature is required and a flattening histogram based on a random walk in the parameter (temperature or energy) space is used to obtain a satisfactory estimation of Z_i. In Refs. [23, 24], the partition function is exactly valued through numerical simulations, taking into account its relationship with the largest eigenvalue $\lambda^{(0)}$ of the transfer matrix $\mathcal{T}$. Although the evaluation of $\lambda^{(0)}$ is possible for lattice-gas systems, its extension for more complex cases (e. g. off-lattice systems) is not straightforward. In contrast to previous "exact" approaches, Park and Pande [25] proposed an approximated tool of estimating weights, based on the average system energy. Since the mean energy is easily obtained for any system (including lattice and off-lattice models), it constitutes a considerable simplification over the free-energy case. Nevertheless, there are some fundamental points that need to be understood in order to make it a promptly useful method. The first one is how this procedure compares itself with using free-energy weights? The second

* fiore@if.usp.br

one is under what conditions does it provide equivalent results to those obtained from free-energy weights? An additional point is if it is possible to obtain proper temperature set that yields precise results under lower computational cost. To answer the aforementioned points, we have analyzed, under the ST with approximated weights, four distinct lattice models, namely, Blume-Capel (BC) and Blume-Emery-Griffiths (BEG) [26], Bell-Lavis (BL) [27, 28] and associating lattice gas (ALG) water models [29, 30]. The former two are interesting tests, due to the existence of very precise results available from cluster algorithms [31], Wang-Landau [32], PT and ST with free-energy weights [14, 18, 19, 33]. Therefore, they constitute relevant benchmarks for our purposes. The BL and ALG are also important examples, taking into account their more complex phase diagrams, including liquid phases with distinct structures, regions of unusual behaviors (density and diffusion anomaly lines) and also dynamic transitions [28, 34]. In the case of ALG, an extra advantage arises, due to the existence of two phase coexisting lines, between gas and liquid phases. Hence, the ALG works as a double checking of reliability of our proposals. For instance, we focus on the regime of low temperatures, in which strong first-order phase transitions separate coexisting phases. Recently a general approach for discontinuous transitions has been proposed [35, 36], in which thermodynamic quantities are described by a general function, allowing to achieve all relevant informations by studying rather small system sizes for some control parameters. Thus, its combination with a proper usage of ST can provide us a powerful approach to deal with discontinuous transitions with rather low computational cost.

Henceforth, the analysis of all cases will show that the approximated weights work properly (and hence lead to correct results) in the regime of large replica numbers R for an appropriate choice of temperature sets [33]. On the other hand, for sufficiently small R its performance is strongly reduced and the system does not visit properly the distinct coexisting regions. Finally we extend for the approximated weights, a simple protocol for obtaining proper temperature sets initially proposed for the free-energy weights [33].

II. SIMULATED TEMPERING AND APPROXIMATED WEIGHTS

The basic idea of the ST concerns with the fact that the system temperature T can assume different values between the extreme values T_1 and T_R, where R is the replica number. The MC simulation is defined as follows: In the first part, starting at a given temperature T_i within the set $\mathcal{T}_R \equiv \{T_1, ..., T_R\}$ (in all cases we started from T_R), a given site of the lattice is randomly chosen and its variable is changed (among all possibilities) according to the Metropolis prescription $\min\{1, \exp(\beta_i \Delta\mathcal{H})\}$, where $\Delta\mathcal{H}(\sigma)$ denotes the energy difference between the "new" and "old" configurations and $\beta_i = 1/k_B T_i$. After repeating above dynamics a proper number of realizations (here L^2 random choices are considered) in the second part the temperature exchange ($T_i \to T_j$) occurs with the following probability

$$p_{i\to j} = \min\{1, \exp[(\beta_i - \beta_j)\mathcal{H}(\sigma) + (g_j - g_i)]\}, \quad (1)$$

where g_i is the weight associated with the temperature T_i and $\mathcal{H}(\sigma)$ is the system Hamiltonian. For a uniform sampling, the weights should be proportional to the free-energy f_i given by $g_i = \beta_i f_i$ [25]. Since the evaluation of f is not an easy task, alternative calculations of weights have been proposed [21–24]. The simplest proposal [25] estimates the g's according to the following approximated formula

$$g_j - g_i \approx (\beta_j - \beta_i)(U_j + U_i)/2, \quad (2)$$

with $U_i = \langle \mathcal{H}_i \rangle$ ($i = 1, 2, \ldots, R$) denoting the average system energy at T_i. Thus, from Eq.(2) the weights are estimated from simple and direct standard numerical simulations. Here we give a further step by analyzing them by inspecting two crucial points: their dependence on the replica number R and on the set of temperatures $\mathcal{T}_R$. In order to scrutinize them, we compare numerical results at the phase coexistence points for distinct R's, with temperature schedules estimated as proposed in Ref. [33] and described as follows: starting from a fixed T_1 we choose the next $R-1$ temperatures $T_2 < T_3 < \ldots < T_R$ in such a way that the resulting exchange frequencies $f_{i+1,i}$ between any two successive temperatures T_i and T_{i+1} are all equal to some value specified $f_{i+1,i} = f$. We define $f_{i+1,i}$ as the ratio of the number of exchanges between T_i and T_{i+1} to the total Monte Carlo steps N_{MC}. Note that from this recipe the highest temperature T_R becomes automatically obtained. The efficiency of such achieved set $\mathcal{T}_R$ is verified by means of standard tests, where in the case of first-order transitions, the tunneling between the coexisting phases and convergence to the steady state starting from a non-typical initial configuration constitute proper efficiency measures. More specifically, the existence of full trapping in a given phase or even temperature changes that do not allow the system to visit properly the coexisting phases will imply in thermodynamic averages marked by no changes or abrupt variations (see e.g Figs. 2 and 3 for $f = 0.02$ and 0.021, respectively). Such points can be understood by recalling the ideas from Ref. [35, 36], when the system close to the phase coexistence have typical thermodynamic quantities, like energy and order parameter, well described by the following general expression

$$W(y) \approx (b_1 + \sum_{n=2}^{\mathcal{N}} b_n \exp[-a_n y])/(1 + \sum_{n=2}^{\mathcal{N}} c_n \exp[-a_n y]), \quad (3)$$

where for $\mathcal{N}$ coexisting phases, y denotes the "distance" to the coexistence point ξ^* given by $y = \xi - \xi^*$. The coefficients c_n's and b_n's are related to derivatives of the

free energies f_n of each phase n with respect to parameter ξ reading $\partial f_n/\partial\xi$ [36]. In the case of two phase coexistence ($\mathcal{N}=2$) Eq. (3) acquires the following way $W(y)=(b_1+b_2\exp[-a_2y])/(1+c_2\exp[-a_2y])$ and hence only four parameters are necessary to determine the whole function. In other words, according to Eq. (3), numerical simulations (of a given system) for known L and control parameter sets $\xi=\xi_0$ (like chemical potential and temperature) will provide a well defined value for thermodynamic quantities $W_0^*=W(L,y_0)$, where $y_0=\xi_0-\xi^*$. Note that at the phase coexistence point $y=0$, the quantity W reads

$$W_0=\frac{b_1+\sum_{n=2}^{\mathcal{N}}b_n}{1+\sum_{n=2}^{\mathcal{N}}c_n} \tag{4}$$

for all L's. Hence, different curves of W should cross at the coexistence point. However, as W_0 and W_0^* are verified only for dynamics that visit properly the distinct phases (e.g. one flip algorithms lead to strong hysteresis at low T's and results do not obey Eq. (3)). In the case of tempering methods, the achievement of results not following Eq. (3) indicates that $\mathcal{T}_R$ is not proper. Typically, low T_i's (including the extreme T_R) provide high temperature exchanges, but the system is not able to cross energy barriers. Hence f should be decreased, in order to raise the temperatures. In contrast, a very high $\mathcal{T}_R$ (obtained from a very low f) may be responsible for few frequent exchanges and hence poor averages are obtained. So that f should be raised, in order to increase the temperature changes. An intermediate optimal frequency f_{opt} is expected to satisfy the above points and hence it may lead to frequent tunneling between the phases and a faster convergence to the steady state. Some remarks are needed: Although our present recipe provides a reliable temperature set, it does not exclude the existence of other optimized choices presenting distinct frequencies between adjacent temperatures. Also, other efficient sets (ranged from T_1 and T_R) can be obtained. For simplicity, we have considered such equal frequencies proposal.

In this work, we will test this procedure for distinct R's, in order to verify the replica number influence in the results. It is worth mentioning that although some numerical work is necessary to find f_{opt}, in practice such process demands relative short simulations. Hence, the search for the corresponding optimal $\mathcal{T}_R$ is not a computationally time consuming procedure.

III. MODELS

A. BEG and BC models

The BEG model Hamiltonian [26] is given by

$$\mathcal{H}=-\sum_{<i,j>}(J\sigma_i\,\sigma_j+K\sigma_i^2\sigma_j^2)+D\sum_i\sigma_i^2, \tag{5}$$

where $\sigma_i=0$, if the site i has null spin and ±1 if i has up and down values, respectively. The parameters J and K are interaction energies and D denotes the crystalline field. The BC model corresponds to the $\bar{K}\equiv K/J=0$ case. In order to compare with previous results [14, 31, 33] we also consider the $\bar{K}=3$ case, in which the system displays ferromagnetic and paramagnetic phases. All phases can be characterized in terms of two order-parameters $q=\langle\sigma_i^2\rangle$ and $m=\langle\sigma_i\rangle$. At low temperatures, all transitions are first-order and yield close to the $T=0$ the value $\bar{D}^*=z(\bar{K}+1)/2$, where z is the coordination number of the lattice. In both model studies, we consider a two-dimensional square lattice in which z reads 4.

B. Bell-Lavis model

The Bell-Lavis (BL) model is defined on a triangular lattice ($z=6$) where each site is described by two kinds of variables, namely occupational (σ) and orientational (τ) states. The former takes the values $\sigma_i=0$ or 1, whenever the site i is empty or occupied by a water molecule, respectively. The latter describes the possibility of forming hydrogen bonds and reads $\tau_i^{ij}=0$ or $\tau_i^{ij}=1$ when the arm is inert or bonding, respectively. Two molecules interact via van der Waals and hydrogen bond energies provided they are adjacent and point out their arms to each other ($\tau_i^{ij}\tau_j^{ji}=1$), respectively. The BL model is given by the following Hamiltonian

$$\mathcal{H}=-\sum_{<i,j>}\sigma_i\,\sigma_j\,(\epsilon_{hb}\,\tau_i^{ij}\,\tau_j^{ji}+\epsilon_{vdw})-\mu\sum_i\sigma_i, \tag{6}$$

where ϵ_{vdw} and ϵ_{hb} are the van der Waals and hydrogen bonds interaction energies, respectively, and μ is the chemical potential. We also compared results with those obtained from PT and ST with free-energy weights [24, 33]. For instance, we consider $\zeta=0.1$ (where $\zeta=\epsilon_{vdw}/\epsilon_{hb}$), in which the system presents a gas and two distinct liquid phases, named low-density-liquid (LDL) and high-density-liquid (HDL) [27, 28]. In the gas and HDL phases, the lattice is empty and it is almost filled by molecules respectively. On the other hand, the LDL phase presents an intermediate density close to $\rho=2/3$ and exhibits an ordering structure (honeycomb like geometry), signed by a maximum density of hydrogen bonds per molecule. At $\bar{T}=0$ (where $\bar{T}\equiv T/\epsilon_{hb}$), both transitions are first-order and occurs at $\bar{\mu}^*=-3\,(1+\zeta)/2$ and $\bar{\mu}^*=-6\,\zeta$, respectively. For $\bar{T}\neq0$ and distinct ζ's the former phase transition remains first-order, but the latter becomes critical [28]. For $\zeta=0.1$, the second-order and first-order lines meet in a tricritical point.

C. Associating lattice-gas (ALG) model

Similarly to the BL, the ALG model is also described by an occupation (σ) and orientation (τ) states. But

an important difference from the BL is that an energetic punishment exists when a hydrogen bond is not formed. More specifically, two first neighbor molecules have an interaction energy of $-v$ ($-v+2u$) if there is (there is not) a hydrogen bond between them. The Hamiltonian system reads

$$\mathcal{H} = 2u \sum_{<i,j>} \sigma_i \sigma_j [(1 - v/(2u)) - \tau_i^{ij} \tau_j^{ji}] - \mu \sum_i \sigma_i. \quad (7)$$

The ALG also presents a gas, LDL and HDL phases, with densities $\rho = 3/4$ and 1, respectively [29]. Another relevant distinction from the BL model is that here both gas-LDL and LDL-HDL transitions remain first-order for $\bar{T} \equiv T/v \neq 0$ and end at respective critical points joined by a critical line separating a structured liquid from a disordered fluid phase. At $\bar{T} = 0$, the discontinuous transitions occur at $\bar{\mu} \equiv \mu/v = -2$ (gas-LDL) and $\bar{\mu} = -6 + 8u/v$ (LDL-HDL). As in the BL model, ρ is a proper parameter for the gas-LDL transition, but not for other phase transitions. Alternative ϕ's are $\phi = (4\rho - 3)$ or also $\phi = (2\rho_{hb} - 3)$, being ρ_{hb} the hydrogen bonds density, taking the values $\rho_{hb} = 3/2$ and 1 for LDL and HDL phases, respectively. Here, we focus on the temperature $\bar{T} = 0.30$, in which results from the PT show that the former and latter transitions take place at $\bar{\mu}^* = -1.9986(2)$ and $\bar{\mu}^* = 2.0000(2)$, respectively [35].

IV. NUMERICAL RESULTS

Numerical simulations were carried out for several system sizes L and control parameters. In all cases, numerical simulations start from a fully ordered initial configuration and 3.10^6 MC steps have been used to "equilibrate" the system. After the transient, we have used 3.10^6 MC steps for evaluating the weights and steady analysis start from the largest temperature T_R. Except Fig. $4(a)$, all quantities have been evaluated after the transient regime. From now on, we will replace all reduced quantities $(\bar{T}, \bar{H}, \bar{D}, \bar{\mu})$ for (T, H, D, μ). In order to achieve a global idea about approximated weights and how they compare with free-energy ones, in the first analysis we show the tunneling between coexisting phases for the BEG and BL models, respectively by taking the temperature schedules $\mathcal{T}_R$ (for distinct R's) obtained from free-energy weights [33]. For low temperature values, $T_1 = 0.5$ (BEG) and 0.1 (BL), the coexistence points yield at $\bar{D}^* = 8.0000(1)$ and $\bar{\mu}^* = -1.6500(1)$, respectively. In these points, according to Eq. (3) a correct system sampling should give steady equilibrium values consistent with $q_0 \approx 2/3$ and $\rho_0 \approx 1/2$ for the BEG and BL, respectively. The former can be understood by recalling that two ferromagnetic phases ($q \approx 1$) coexist with one paramagnetic phase ($q \approx 0$). Since at the phase coexistence their weights are equal (1/3), we have $q_0 \approx 2/3$ for all L's. A similar reasoning holds for the latter model, in which the LDL phase has density $\rho \approx 2/3$ (with degeneracy 3) and coexist with the gas phase, in such a way that at $\bar{\mu}^*$ the value $\rho_0 \approx 1/2$ is verified. For this study, three values of R and frequencies were considered, whose temperature sets and distinct f's are obtained from free-energy weights and are shown in Tables I, II and III (BEG) and Tables IV,V and VI (BL). Results are summarized in Figs. 1 and 2 for $L = 20$ and $L = 18$, respectively. As discussed previously, in all cases extremely low or large frequencies provide no precise results, signaling trapping in a given phase ($q = 0$ or 1 for the BEG and $\rho = 0$ and 2/3 for the BL), due to low T's or hardly exchanges. However, a similar result is verified for the intermediate f and the lowest $R = 3$, in such a way that only for intermediate frequencies ($f = f_{opt}$) when $R = 6$ and $R = 8$, the crossing between coexisting phases is verified. However, for $R = 6$ the averages deviate greatly from its mean value 2/3, indicating that despite tunneling between coexisting phase occurs, it is not efficient. Improved results are obtained only for f_{opt} and $R = 8$, in which the tunneling is more frequent. These results present stark difference with those obtained by taking the free-energy weights (insets), in which for all replica numbers (including the lowest $R = 3$ case), it is possible to find an optimal f_{opt}, ensuring proper tunneling between phases. Thus, the first evidence suggests that the choice of the replica number R is more important with approximated weights than with the free-energy ones.

The results for the BL shown in Fig. 2 reinforce this idea. Only for the largest case $R = 6$ with $f = f_{opt}$, some tunneling between the gas and LDL phases occurs. As for the BEG model, free-energy weights provide reliable results for all R's (insets). The crucial importance of R is understood as follows: For two arbitrarily temperatures T_i and T_j the exchange frequency obtained from the

f	5×10^{-2}	6×10^{-4} (f_{opt})	10^{-5}
T_1	0.50	0.50	0.50
T_2	1.35	1.60	1.82
T_3	1.70	2.05	2.33

TABLE I. Temperature sets $\mathcal{T}_{R=3}$, for BEG model, considering the frequencies f obtained from free-energy weights [33].

f	0.37	0.11 (f_{opt})	10^{-4}
T_1	0.50	0.50	0.50
T_2	1.12	1.25	1.70
T_3	1.24	1.55	2.14
T_4	1.34	1.78	3.20
T_5	1.42	1.95	4.34
T_6	1.50	2.06	6.10

TABLE II. Temperature sets $\mathcal{T}_{R=6}$, for the BEG model, considering distinct frequencies f obtained from free-energy weights [33].

f	0.37	0.21 (f_{opt})	10^{-4}
T_1	0.50	0.50	0.50
T_2	1.12	1.16	1.70
T_3	1.24	1.39	2.14
T_4	1.34	1.56	3.20
T_5	1.42	1.72	4.34
T_6	1.50	1.85	6.10
T_7	1.58	1.96	6.60
T_8	1.64	2.03	7.00

TABLE III. Temperature sets $\mathcal{T}_{R=8}$, for the BEG model, considering distinct frequencies f obtained from free-energy weights [33].

f	0.025	2×10^{-4} (f_{opt})	10^{-5}
T_1	0.10	0.10	0.10
T_2	0.25	0.32	0.35
T_3	0.33	0.43	0.48

TABLE IV. Temperature sets $\mathcal{T}_{R=3}$, for the BL model, considering distinct frequencies f obtained from free-energy weights [33].

approximated weights is lower than those from the free-energy ones, whose difference becomes more pronounced for the optimal choices. For example, for the BEG and $R = 3$ the exchange between $T_1 = 0.50$ and $T_2 = 1.60$ (Table I) is performed with frequency $f_{opt} = 6.10^{-4}$ when one takes the free-energy weights. For the approximated weights, it reads 10^{-6}. An efficient performance of the ST (e.g. the system visiting properly distinct coexisting phases) depends not only on frequent exchanges but also a reliable estimation of all temperature schedules, including the extreme temperature T_R. Thus, the compromise between these points is reached (by taking the approximated weights) only for larger R's. For example, in such regime (exemplified here for $R = 8$) the exchange between $T_1 = 0.50$ and $T_2 = 1.16$ (Table III) is performed with a considerable larger frequency, reading $f = 0.21$ and $f = 0.015$ when one takes the free-energy and approximated weights, respectively. We remark that frequency 0.015 is larger than the value 10^{-6} obtained be-

f	0.15	0.01 (f_{opt})	1.5×10^{-3}
T_1	0.10	0.10	0.10
T_2	0.20	0.27	0.29
T_3	0.25	0.34	0.39
T_4	0.29	0.43	0.50

TABLE V. Temperature sets $\mathcal{T}_{R=4}$, for the BL model, considering distinct frequencies f obtained from free-energy weights [33].

f	0.37	0.07 (f_{opt})	0.02
T_1	0.100	0.10	0.10
T_2	0.200	0.23	0.25
T_3	0.230	0.30	0.32
T_4	0.260	0.32	0.41
T_5	0.285	0.39	0.47
T_6	0.312	0.43	0.60

TABLE VI. Temperature sets $\mathcal{T}_{R=6}$, for the BL model, considering distinct frequencies f obtained from free-energy weights [33].

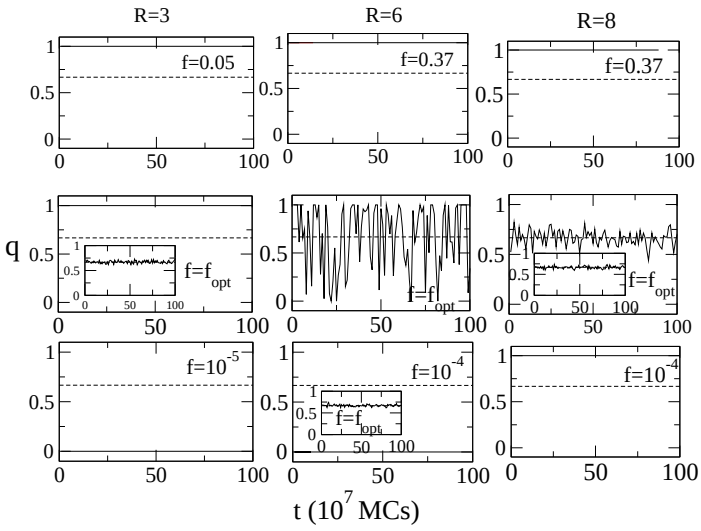

FIG. 1. Order parameter q as a function of t for the BEG model at $T = 0.5$ for $L = 20$. Distinct values of f's and R's were considered at the phase coexistence $D^* = 8.0000(1)$, with temperature sets obtained from Ref. [33] but using the approximated weights. The dashed lines correspond to steady value $q_0 = 2/3$. The insets correspond to the results from free-energy weights.

tween 0.5 and 1.60 (approximated weights). For the BEG model, in Fig. 3 we confirm these points by obtaining temperature schedules $\mathcal{T}_R$'s (for $R = 6$ and $R = 8$) with frequencies evaluated from the approximated weights, instead of those available from free-energy values [33]. As in previous cases, three frequencies have been considered, with temperature sets shown in Tables VII and VIII for $R = 6$ and $R = 8$, respectively. As in Fig. 1, larger f's provide more frequent exchanges, but it is not efficient since the obtained T_R is low. On the contrary, lower f gives a larger T_R but temperatures exchanges are hardly performed (clearly shown for the lowest $f = 0.021$ when $R = 6$). By increasing R, it becomes possible to obtain an intermediate frequency f_{opt} that fulfills the two requirements above for an efficient performance (larger T_R and frequent temperature exchanges).

Fig. $4(a)$ reinforces above ideas by showing for the BEG model the time decay of the order-parameter q

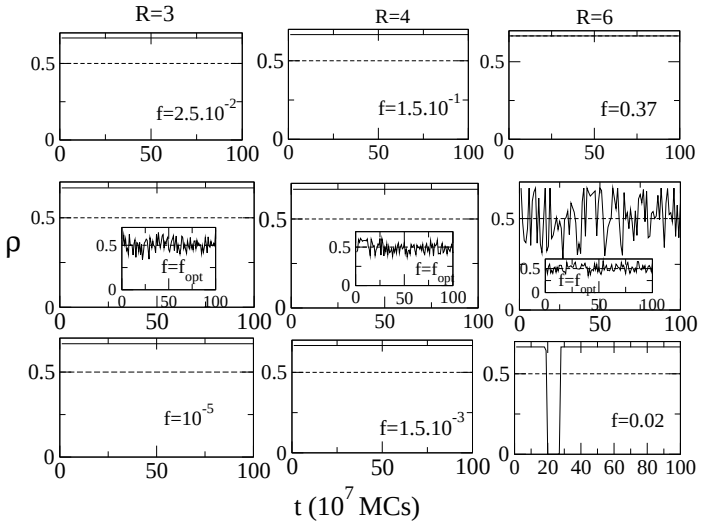

FIG. 2. For the BL model and $T = 0.1$, ρ vs t for the BL model at the phase coexistence $\mu^* = -1.6500(1)$ for distinct R's and f's, with temperature sets obtained from Ref. [33] but using the approximated weights. Numerical simulations have been carried out for $L = 18$. The dashed lines denote the steady density $\rho_0 = 1/2$ and the insets correspond to the free-energy weights.

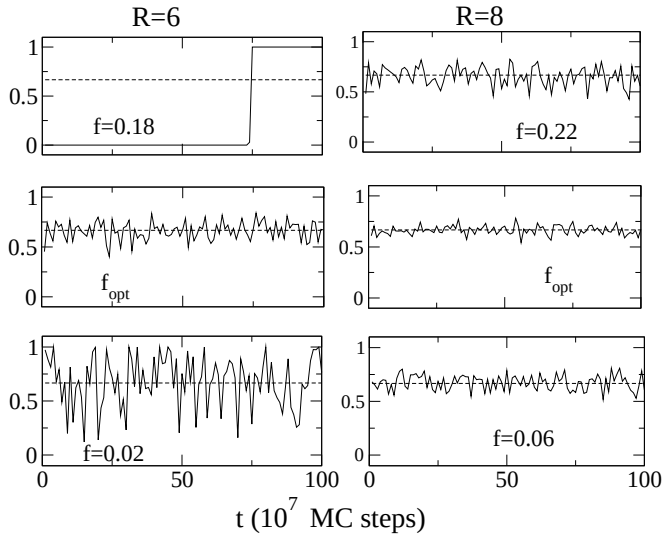

FIG. 3. For the BEG model, $T = 0.5$ and $L = 20$, q versus t for distinct f's and R's at the phase coexistence $D^* = 8.0000(1)$, whose sets are obtained from approximated weights. The dashed lines correspond to steady value $q_0 = 2/3$.

f	0.18	0.06 (f_{opt})	0.02
T_1	0.50	0.50	0.50
T_2	1.02	1.10	1.15
T_3	1.31	1.48	1.58
T_4	1.53	1.77	1.88
T_5	1.68	1.97	2.08
T_6	1.83	2.12	2.47

TABLE VII. Temperature sets $\mathcal{T}_{R=6}$, for the BEG model, considering distinct frequencies f obtained from the approximated weights.

f	0.22	0.10 (f_{opt})	0.06
T_1	0.50	0.50	0.50
T_2	1.00	1.07	1.10
T_3	1.27	1.42	1.48
T_4	1.47	1.68	1.77
T_5	1.63	1.87	1.97
T_6	1.77	2.01	2.12
T_7	1.89	2.15	2.44
T_8	1.98	2.43	3.03

TABLE VIII. Temperature sets $\mathcal{T}_{R=8}$, for the BEG model, considering distinct frequencies f obtained from the approximated weights.

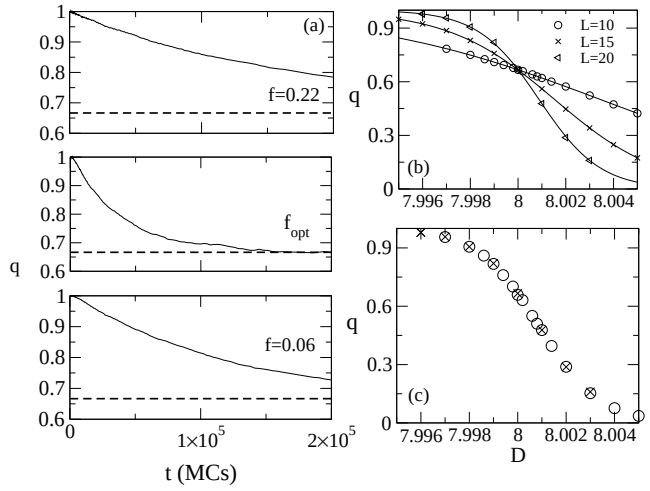

FIG. 4. For the BEG model, panel (a) shows the time decay of the order-parameter q for distinct f's at the phase coexistence $D^* = 8.0000(1)$ for $R = 8$ and $L = 20$. In (b) q vs D for distinct L's, with numerical results obtained from $\mathcal{T}_{R=8}$ for f_{opt}. The continuous lines denote results for q obtained from Eq. (3). In (c) we compare results with those obtained from approximated (stars) and free-energy (circles) weights.

starting from a fully occupied initial configuration for distinct f's and $R = 8$. Note that the optimal choice f_{opt} also ensures the faster convergence toward the steady value 2/3. In panel (b) we extend the obtained $\mathcal{T}_{R=8}$ (for the coexistence point D^*) for other D's and distinct system sizes. As for free-energy case [14, 33], an unique $\mathcal{T}_R$'s can be used for other control parameters and system sizes (panel (c)), providing to characterize very precisely the transition point, as predicted by Eq. (3) by taking only

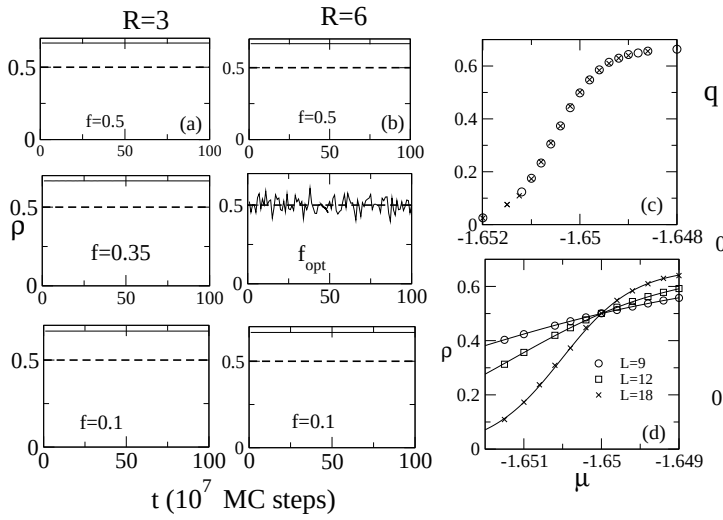

FIG. 5. In (a) and (b), ρ versus t for distinct values of f's and R's at the phase coexistence point ($T = 0.1$, $\mu^* = -1.6500(1)$) for the BL model and $L = 18$. The dashed lines denote the steady density $\rho_0 = 1/2$. From top to bottom, intermediate temperature schedules read $\{0.183, 0.230\}$, $\{0.200, 0.266\}$ and $\{0.30, 0.40\}$ ($R = 3$) and $\{0.183, 0.230, 0.273, 0.312, 0.348\}$, $\{0.200, 0.266, 0.322, 0.372, 0.412\}$ and $\{0.300, 0.400, 0.445, 0.526, 0.670\}$ ($R = 6$). In (c) we compare with results obtained from free-energy weights (circles). In (d) ρ versus μ for distinct system sizes for $T = 0.1$. The continuous lines denote results for ρ obtained from Eq. (3).

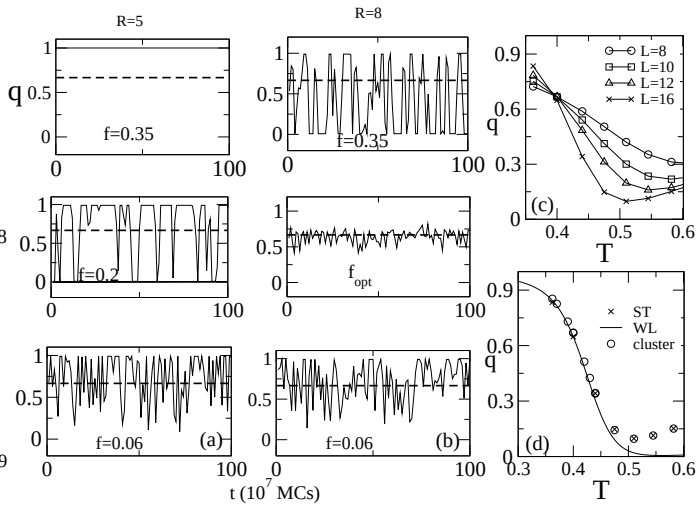

FIG. 6. For the BC model, panels (a) and (b), q versus t for distinct values of f's and R's at the phase coexistence point ($T = 0.40$, $D^* = 1.9968$) for $L = 16$. The dashed lines denote the steady value $q_0 = 2/3$. In (c) we plot q vs T for distinct L's. The curves cross at the transition point $T = 0.40(1)$. In (d), we compare results obtained from the WL method and cluster algorithms.

small system sizes.

In Fig. 5 we compare distinct $\mathcal{T}_R$'s for the BL model, by taking approximated weights. Confirming previous results, the optimal frequency f_{opt} is obtained only by increasing R (panels (a) and (b)) with results equivalent with the free-energy weights (panel (c)). As for the BEG model, the same $\mathcal{T}_R$ is extended to values of μ and system sizes, as shown in panel (d) with results obeying Eq. (3).

Next, we analyze the BC model. Besides testing the previous ideas, such analysis also aims to consider a phase transition ruled by the temperature. Thus, it also shows the reliability of the whole temperature set obtained from f_{opt}. We take the value $D^* = 1.9968$, in which results from the cluster algorithms [6], WL method [32] and PT [18] predicts a phase coexistence close to $T = 0.4$. Results for the tunneling between coexisting phases are considered for $L = 16$, as shown in Fig. 6. From top to bottom panels, temperature schedules read $\{0.375, 0.400, 0.420, 0.440, 0.458\}$, $\{0.350, 0.400, 0.440, 0.485, 0.527\}$ and $\{0.310, 0.400, 0.481, 0.560, 0.650\}$ ($R = 5$) and $\{0.375, 0.400, 0.420, 0.440, 0.458, 0.480, 0.509, 0.530\}$, $\{0.350, 0.400, 0.440, 0.485, 0.527, 0.570, 0.619, 0.680\}$ and $\{0.310, 0.400, 0.481, 0.560, 0.650, 0.783, 0.985, 1.290\}$ ($R = 8$). As in previous examples, small R leads to trapping of the system with the method performance improving as R increases. As it can be seen, the achievement of an optimal $\mathcal{T}_R$ ensures tunneling and faster convergence toward the equilibrium value. Also, the same $\mathcal{T}_R$ is extended for distinct L's and from Eq. (3) we see that all curves cross at $T = 0.40(1)$ (panel (c)). For $T > 0.5$, we see an unusual behavior, signaling the large temperature regimes and the non-validity of Eq. (3). Comparison with cluster algorithms [6] and WL results [32] (panel (d)) confirms once again the main ideas that approximate weights can be used properly in order to give results equivalent with such tools.

For the last example, Figs. 7 and 8 summarize results for the ALG model by taking the gas-LDL and LDL-HDL coexistence points for $T = 0.30$. In such cases, one expects steady values close to $\rho_0 \approx 3/5$ and $\phi_0 \approx 0.425$, respectively. The former value can be understood by recalling the LDL phase has density $\rho = 3/4$ and degeneracy 4 and coexists with the gas phase. Since their weights are equal $(1/5)$ at the phase coexistence, the steady $\rho_0 \approx 3/5$ is verified. The latter value is not easily understood, since the HDL phase is highly degenerated. Results for the tunneling between coexisting phases are shown for $L = 12$. As in all previous cases, extreme frequencies give results deviating from steady values, whereas the optimal frequency is signed for proper crossing between phases with accuracy improving as R increases. However, in such case each transition point study requires its own temperature schedule, since the gas-LDL coexistence line is shorter than the LDL-HDL, ending at respective distinct critical temperatures $T_c = 0.55$ and 0.825, respectively [29]. For each $\mathcal{T}_R$ we obtain the thermodynamic quantities, as shown in parts $7(c)$ and 8 (c). Note that

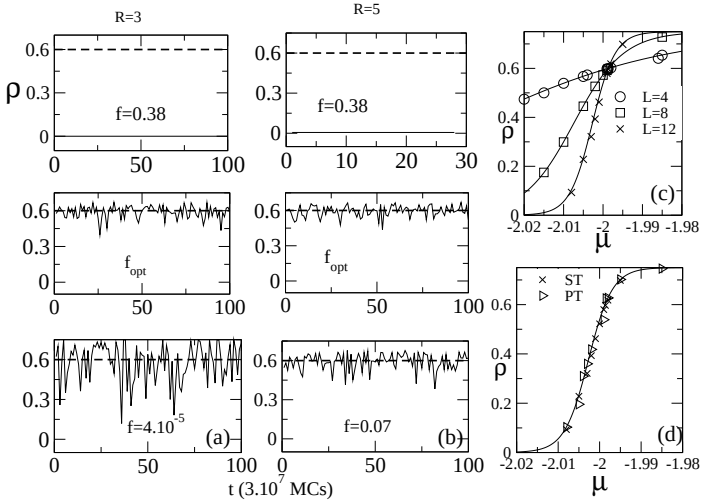

FIG. 7. For the ALG model and $L = 12$, panels (a) and (b) show ρ versus t for distinct values of f's and R's at the gas-LDL phase coexistence point $\mu^* = -1.9986(1)$ and $T = 0.30$. The dashed lines denote the steady density $\rho_0 = 3/5$. From top to bottom, intermediate temperature schedules read $\{0.32, 0.34\}$, $\{0.406, 0.520\}$ and $\{0.44, 0.56\}$ $(R = 3)$ and $\{0.32, 0.34, 0.355, 0.372\}$, $\{0.355, 0.395, 0.434, 0.473\}$ and $\{0.38, 0.45, 0.53, 0.653\}$ $(R = 5)$. In (c) ρ versus μ for distinct system sizes. The continuous lines denote results for ρ obtained from Eq. (3). In (d) we compare with results obtained from the PT (triangles) for $L = 12$.

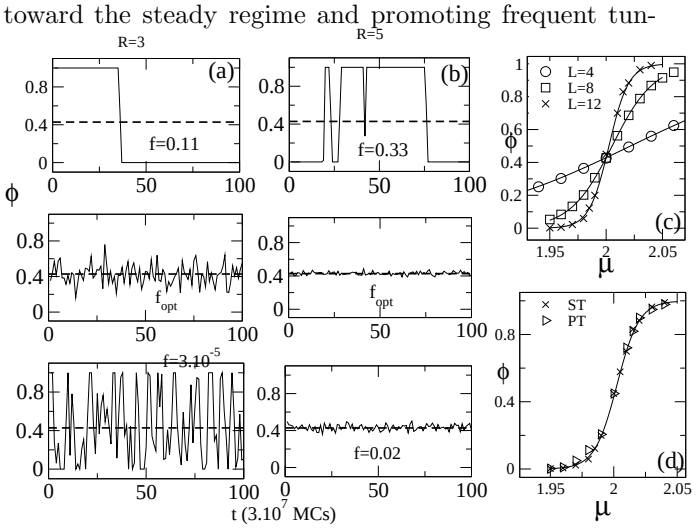

FIG. 8. For the ALG model and $L = 12$, panels (a) and (b) show ϕ versus t for distinct values of f's and R's at the LDL-HDL phase coexistence point $\mu^* = 2.000(1)$ and $T_1 = 0.30$. The dashed lines denote the steady density $\phi_0 = 0.425$. From top to bottom, intermediate temperature schedules read $\{0.55, 0.70\}$, $\{0.60, 0.78\}$ and $\{0.65, 0.84\}$ $(R = 3)$ and $\{0.50, 0.579, 0.650, 0.705\}$, $\{0.55, 0.70, 0.795, 0.840\}$ and $\{0.60, 0.78, 0.89, 1.20\}$ $(R = 5)$. In (c) ϕ versus μ for distinct system sizes. The continuous lines denote results for ϕ obtained from Eq. (3). In (d) we compare with results obtained from the PT (triangles) for $L = 12$.

results are fully described by Eq. (3) (continuous lines). Also, both panels (d) show the equivalence of results with those obtained from the PT [35]. However, larger replica numbers and non adjacent replica exchanges were required for the system visiting properly the phases when the PT is considered [35].

V. DISCUSSION AND CONCLUSION

Simulated tempering with approximated weights, proposed by Park et. al. [25], presents a great advantage over other procedures, since the achievement of weights is readily obtained by executing simple and standard numerical simulations. Aimed at unveiling and optimizing its performance, we scrutinized their main points focusing in the regime of first-order transitions at low temperatures, in which the existence of large trapping in metastable states makes the improvement of approximated weights a highly desired problem. Four systems having available results from parallel tempering, simulated tempering with free-energy weights, Wang-Landau method and cluster algorithms have been considered and thus they are important benchmarks for testing all obtained results.

In all cases, results showed that approximated weights improves the efficiency of the ST as the replica number increases and optimized sets accelerating the convergence toward the steady regime and promoting frequent tunneling between coexisting phases have been found. We remark that the minimum value R ensuring proper sampling may depend on the system size and also the system temperature studied. We believe that the proposed recipe for the ST with approximated weights combined with Eq. (3) provides a very powerful method for dealing with discontinuous transitions, demanding relative short systems (as those considered here) and few control parameters [35, 36]. Although not necessary (in conformity with the main ideas concerning Eq. (3)), the extension for larger system sizes is straightforward. However, larger replica numbers or non-adjacent replica exchanges can be required. As a final comment, we remark that future method extensions include polymeric models and off-lattice systems, in which tempering methods have been extensively exploited, but the achievement of free-energy weights is difficult. These points should be addressed in future works.

VI. ACKNOWLEDGMENTS

CEF acknowledges the financial support from CNPQ.

[1] K. Binder and D. W. Heermann, Monte Carlo Simulation in Statistical Physics (Springer-Verlag, New York Berlin Heidelberg, 1992).

[2] N. Metropolis, A. W. Rosenbluth, M. N. Rosenbluth and A. H. Teller, J. Chem. Phys. **21**, 1087 (1953).

[3] K. Binder and W. Kob, *Glassy Materials and Disordered Solids: An Introduction to their Statistical Mechanics* (World Scientific, Singapoure, 2005).

[4] J. Skolnick and A. Kolinski, Comput. Sci. Eng. **3**(9/10), 40 (2001).

[5] R. H. Swendsen and J. S. Wang, Phys. Rev. Lett. **58**, 86 (1987), U. Wolff, Phys. Rev. Lett **62**, 361 (1989).

[6] M. Bouabci and C. E. I. Carneiro, Phys. Rev. B **54**, 359 (1996).

[7] B. A. Berg and T. Neuhaus, Phys. Lett. B **267**, 249 (1991); Phys. Rev. Lett. **68**, 9 (1992).

[8] F. Wang and D. P. Landau, Phys. Rev. Lett. **86**, 2050 (2001); Phys. Rev. E **64**, 056101 (2001).

[9] K. Hukushima and K. Nemoto, J. Phys. Soc. Jpn. **65**, 1604 (1996).

[10] E. Marinari and G. Parisi, Europhys. Lett. **19**(6), 451 (1992).

[11] A. Kone and D. A. Kofke, J. Chem. Phys **122**, 206101 (2005).

[12] H. G. Katzgraber, S. Trebst, D. A. Huse and M. Troyer, J. Stat. Mech. **3**, P031018 (2006).

[13] D. Sabo, M. Meuwly, D. L. Freeman and J. D. Doll, J. Chem. Phys **128**, 174109 (2008).

[14] C. E. Fiore, J. Chem. Phys **135**, 114107 (2011).

[15] J. P. Neirotti, F. Calvo, D. L. Freeman and J. D. Doll, J. Chem. Phys. **112**, 10340 (2000).

[16] F. Calvo, J. P. Neirotti, D. L. Freeman and J. D. Doll, J. Chem. Phys. **112**, 10350 (2000).

[17] F. Calvo, J. Chem. Phys. **123**, 124106 (2005).

[18] C. E. Fiore, Phys. Rev. E **78**, 041109 (2008).

[19] C. E. Fiore and M. G. E. da Luz, Phys. Rev. E **82**, 031104 (2010).

[20] E. Rosta and G. Hummer, J. Chem. Phys. **131**, 165102 (2009); J. Chem. Phys. **132**, 034102 (2010).

[21] C. Zhang and J. P. Ma, J. Chem. Phys, **129**, 134112 (2008).

[22] C. Zhang and J. P. Ma, Phys. Rev. E **76**, 036708 (2007).

[23] R. A. Sauerwein and M. J. de Oliveira, Phys. Rev. B, **52**, 3060 (1995).

[24] C. E. Fiore and M. G. E. da Luz, J. Chem. Phys **133**, 104904 (2010).

[25] S. Park and V. S. Pande, Phys. Rev. E **76**, 016703 (2007).

[26] M. Blume, V. J. Emery, and R. B. Griffiths, Phys. Rev. A **4**, 1071 (1971), W. Hoston and A. N. Berker, Phys. Rev. Lett. **67**, 1027 (1991).

[27] G. M. Bell and D. A. Lavis, J. Phys. A **3**, 568 (1970).

[28] C. E. Fiore, M. M. Szortyka, M. C. Barbosa and V. B. Henriques, J. Chem. Phys **131**, 164506 (2009).

[29] A. L. Balladares, V. B. Henriques, and M. C. Barbosa, J. Phys. C **19**, 116105 (2007).

[30] V. B. Henriques and M. C. Barbosa, Phys. Rev. E **71**, 031504 (2005).

[31] C. E. Fiore and C. E. I. Carneiro, Phys. Rev. E **76**, 021118 (2007).

[32] C. J. Silva, A. A. Caparica and J. A. Plascak, Phys. Rev. E **73**, 036702 (2006).

[33] A. Valentim, M. G. E. da Luz and C. E. Fiore, Comp. Phys. Comm. **128**, 2046 (2014).

[34] M. M. Szortyka, C. E. Fiore, V. B. Henriques and M. C. Barbosa, J. Chem. Phys **133**, 104904 (2010).

[35] C. E. Fiore, M. G. E. da Luz, Phys. Rev. Lett. 107 230601, (2011).

[36] C. E. Fiore, M. G. E. da Luz, J. Chem. Phys. 138 014105, (2013).

[37] B. Kaufman, Phys. Rev. **76**, 1232 (1949); A. E. Ferdinand and M. E. Fisher, Phys. Rev. **185**, 832 (1969).